Title

Experimental demonstration of bandwidth enhancement based on two-pump wavelength conversion in a silicon waveguide

Journal

Optics Express, 18(26)

ISSN

1094-4087

Authors

Gao, Shiming
Tien, En-Kuang
Huang, Yuewang
et al.

Publication Date

2010-12-17

DOI

10.1364/OE.18.027885

Experimental demonstration of bandwidth enhancement based on two-pump wavelength conversion in a silicon waveguide

Shiming Gao,[1,2,*] En-Kuang Tien,[2] Yuewang Huang,[2] and Sailing He[1]

[1]*Centre for Optical and Electromagnetic Research, State Key Laboratory of Modern Optical Instrumentation, Zhejiang University, Hangzhou 310058, China*

[2]*Advanced Photonics Device and System Laboratory, Department of Electrical Engineering and Computer Science, University of California, Irvine, California 92697, USA*

**gaosm@zju.edu.cn*

Abstract: We experimentally demonstrate the bandwidth enhancement of wavelength conversion in a silicon waveguide based on four-wave mixing (FWM) with two continuous-wave pumps. Our measurement results show 25% bandwidth improvement from 29.8 nm to 37.4 nm in a 17-mm-long silicon waveguide with a pump spacing of 14.9 nm as compared to a single-pump FWM. The experimental results are verified by theoretical calculations and >40% bandwidth enhancement is predicted by further wavelength separation of the two pumps.

OCIS codes: (190.4380) Nonlinear optics, four-wave mixing; (190.4390) Nonlinear optics, integrated; (130.7405) Wavelength conversion devices.

References and links

1. K. K. Chow, C. Shu, C. Lin, and A. Bjarklev, "Polarization-insensitive widely tunable wavelength converter based on four-wave mixing in a dispersion-flattened nonlinear photonic crystal fiber," IEEE Photon. Technol. Lett. **17**(3), 624–626 (2005).
2. R. Jiang, R. Saperstein, N. Alic, M. Nezhad, C. McKinstrie, J. Ford, Y. Fainman, and S. Radic, "Parametric wavelength conversion from conventional near-infrared to visible band," IEEE Photon. Technol. Lett. **18**(23), 2445–2447 (2006).
3. S. Gao, C. Yang, and G. Jin, "Flat broad-band wavelength conversion based on sinusoidally chirped optical superlattices in lithium niobate," IEEE Photon. Technol. Lett. **16**(2), 557–559 (2004).
4. S. Gao, C. Yang, X. Xiao, Y. Tian, Z. You, and G. Jin, "Bandwidth enhancement and response flattening of cascaded sum- and difference-frequency generation-based wavelength conversion," Opt. Commun. **266**(1), 296–301 (2006).
5. X. Sang, and O. Boyraz, "Gain and noise characteristics of high-bit-rate silicon parametric amplifiers," Opt. Express **16**(17), 13122–13132 (2008), http://www.opticsinfobase.org/abstract.cfm?URI=oe-16-17-13122.
6. S. Gao, X. Zhang, Z. Li, and S. He, "Polarization-independent wavelength conversion using an angled-polarization pump in a silicon nanowire waveguide," IEEE J. Sel. Top. Quantum Electron. **16**(1), 250–256 (2010).
7. H. Rong, Y.-H. Kuo, A. Liu, M. Paniccia, and O. Cohen, "High efficiency wavelength conversion of 10 Gb/s data in silicon waveguides," Opt. Express **14**(3), 1182–1188 (2006), http://www.opticsinfobase.org/abstract.cfm?URI=oe-14-3-1182.
8. K. Yamada, H. Fukuda, T. Tsuchizawa, T. Watanabe, T. Shoji, and S. Itabashi, "All-optical efficient wavelength conversion using silicon photonic wire waveguide," IEEE Photon. Technol. Lett. **18**(9), 1046–1048 (2006).
9. B. G. Lee, A. Biberman, A. C. Turner-Foster, M. A. Foster, M. Lipson, A. L. Gaeta, and K. Bergman, "Demonstration of broadband wavelength conversion at 40 Gb/s in silicon waveguides," IEEE Photon. Technol. Lett. **21**(3), 182–184 (2009).
10. X. Zhang, S. Gao, and S. He, "Optimal design of a silicon-on-insulator nanowire waveguide for broadband wavelength conversion," Prog. Electromagn. Res. **89**, 183–198 (2009).
11. Q. Lin, J. Zhang, P. M. Fauchet, and G. P. Agrawal, "Ultrabroadband parametric generation and wavelength conversion in silicon waveguides," Opt. Express **14**(11), 4786–4799 (2006), http://www.opticsinfobase.org/oe/abstract.cfm?URI=oe-14-11-4786.
12. A. C. Turner, C. Manolatou, B. S. Schmidt, M. Lipson, M. A. Foster, J. E. Sharping, and A. L. Gaeta, "Tailored anomalous group-velocity dispersion in silicon channel waveguides," Opt. Express **14**(10), 4357–4362 (2006), http://www.opticsinfobase.org/oe/abstract.cfm?URI=oe-14-10-4357.
13. X. Liu, W. M. J. Green, X. Chen, I.-W. Hsieh, J. I. Dadap, Y. A. Vlasov, and R. M. Osgood, Jr., "Conformal dielectric overlayers for engineering dispersion and effective nonlinearity of silicon nanophotonic wires," Opt. Lett. **33**(24), 2889–2891 (2008).

#137992 - $15.00 USD Received 10 Nov 2010; revised 3 Dec 2010; accepted 6 Dec 2010; published 17 Dec 2010

14. A. C. Turner-Foster, M. A. Foster, R. Salem, A. L. Gaeta, and M. Lipson, "Frequency conversion over two-thirds of an octave in silicon nanowaveguides," Opt. Express **18**(3), 1904–1908 (2010), http://www.opticsinfobase.org/oe/abstract.cfm?URI=oe-18-3-1904.
15. S. Gao, E.-K. Tien, Q. Song, Y. Huang, and O. Boyraz, "Ultra-broadband one-to-two wavelength conversion using low-phase-mismatching four-wave mixing in silicon waveguides," Opt. Express **18**(11), 11898–11903 (2010), http://www.opticsinfobase.org/abstract.cfm?URI=oe-18-11-11898.
16. J. S. Park, S. Zlatanovic, M. L. Cooper, J. M. Chavez-Boggio, I. B. Divliansky, N. Alic, S. Mookherjea, and S. Radic, "Two-pump four-wave mixing in silicon waveguides," in *Frontiers in Optics, OSA Tech. Dig.*, San Jose, CA, 2009, paper FML2.
17. S. Gao, Z. Li, E.-K. Tien, S. He, and O. Boyraz, "Performance evaluation of nondegenerate wavelength conversion in a silicon nanowire waveguide," J. Lightwave Technol. **28**(21), 3079–3085 (2010).
18. S. Gao, Z. Li, E.-K. Tien, Q. Liu, S. He, and O. Boyraz, "Broadband wavelength conversion by nondegenerate four-wave mixing in a silicon-on-insulator waveguide," in *Tech. Dig., Integr. Photon. Res. Conf.*, Monterey, CA, 2010, paper IWC2.
19. D. Dimitropoulos, R. Jhaveri, R. Claps, J. C. S. Woo, and B. Jalali, "Lifetime of photogenerated carriers in silicon-on-insulator rib waveguides," Appl. Phys. Lett. **86**(7), 071115 (2005).

1. Introduction

Wavelength conversion based on wave mixing in nonlinear media such as highly nonlinear fibers, ferroelectric crystals, and semiconductor optical amplifiers is considered as a promising solution for the next generation dense wavelength-division-multiplexing systems, due to its all-optical, high-speed, and data-format transparent characteristics. In such kind of wavelength converters, the conversion bandwidth is one of the most important figures of merit and is mainly dominated by the phase-matching condition of the involved wave-mixing effect. Many efforts have been made to enhance the conversion bandwidth by decreasing the phase mismatch, such as using special dispersion-flattened fibers [1], short highly nonlinear fibers [2], aperiodic quasi-phase-matching structures [3] or cascaded sum-frequency and difference-frequency generation in nonlinear crystals [4]. Recently, four-wave mixing (FWM) in silicon waveguides emerged and became a new promising way to realize integrated planar wavelength converters because of the excellent nonlinear Kerr characteristic and sophisticated fabrication technology of silicon [5–9]. Meanwhile, some efforts were also made to enhance the bandwidth. An effective way to do so is to decrease the FWM phase mismatch by optimizing waveguide geometries [10–12] or designing waveguide structures [13,14]. Turner-Foster *et al.* demonstrated a bandwidth of more than 800 nm with an efficiency fluctuation of less than 10 dB in a dispersion-optimized silicon waveguide [14]. As proposed before in quasi-phase-matching crystals, the bandwidth can be efficiently enhanced using two pumps since the phase-matching condition can then be flexibly controlled [3]. In silicon waveguides, two-pump FWM has already been used to realize one-to-two wavelength conversion [15] or to generate multiple mixing sidebands [16]. In our previous work, we have theoretically analyzed the enhancement in conversion bandwidth of the wavelength conversion using two-pump FWM in a silicon waveguide [17,18]. In this paper, we experimentally demonstrate the bandwidth enhancement of the two-pump wavelength conversion. The 3-dB bandwidth is measured to be 37.4 nm in a 17-mm-long silicon waveguide and the bandwidth enhancement is demonstrated by comparing it to the single-pump FWM (29.8 nm). Analysis shows that more bandwidth enhancement can be achieved through further separating the two-pump wavelengths or engineering the dispersion profile of the used silicon waveguide.

2. Experimental setup and results

The experimental setup is shown in Fig. 1. The two pumps are provided by two continuous-wave (cw) tunable lasers (Santec ECL-200) whose wavelengths are set at 1549.9 and 1564.8 nm. They are coupled through a 50/50 coupler and amplified using a high-power erbium-doped fiber amplifier (Amonics AEDFA-C-33-R), whose saturation power is around 23 dBm. The two pumps are filtered out through a demultiplexer whose central wavelength is at 1550 nm and a tunable band-pass filter, which is tuned to about 1565 nm. Another cw tunable laser (ECL-210) serves as the signal, whose output power is about 11 dBm. The pumps and signal are coupled into a 17-mm-long silicon waveguide with a cross section of 3 μm × 3 μm (the effective mode area is about 5 μm^2) via a 70/30 coupler. After this coupler, the powers of the

#137992 - $15.00 USD Received 10 Nov 2010; revised 3 Dec 2010; accepted 6 Dec 2010; published 17 Dec 2010

two pumps and the signal are estimated to be around 13.2, 19.8, and 6.1 dBm, respectively. The coupling efficiency between the fiber and the waveguide is about 1.5 dB. In the silicon waveguide, FWM occurs among the two pumps and the signal, and an idler is generated at $f_i = f_{p1} + f_{p2} - f_s$ while $f_{p1,p2,s,i}$ represents the frequencies of the involved waves. The FWM spectrum is observed using an optical spectrum analyzer (Ando AQ6317B).

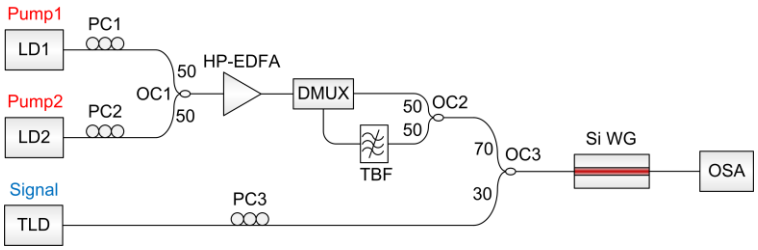

Fig. 1. Experimental setup for the wavelength conversion based on two-pump FWM. TLD: tunable laser diode, PC: polarization controller, EDFA: erbium-doped fiber amplifier, TBF: tunable bandwidth filter, OC: optical coupler, and OSA: optical spectrum analyzer.

Figure 2(a) shows the measured optical spectrum of the two-pump wavelength conversion using the experimental setup in Fig. 1. Here the signal is set at 1561.4 nm and the idler is generated at 1553.2 nm, which is enlarged and shown in the inset. From Fig. 2(a), one can find that the extinction ratio of the generated idler, which is defined as the difference between peak power and the noise floor, is about 10 dB with a measured resolution of 0.01 nm. For comparison, the FWM with a single pump is also experimentally demonstrated. Here Pump1 is turned off and Pump2 is tuned to 1557.7 nm, almost equal to the central wavelength of the two pumps in the two-pump FWM. As shown in Fig. 2(b), a signal at 1561.5 nm is converted to 1553.9 nm pumped by the single Pump2.

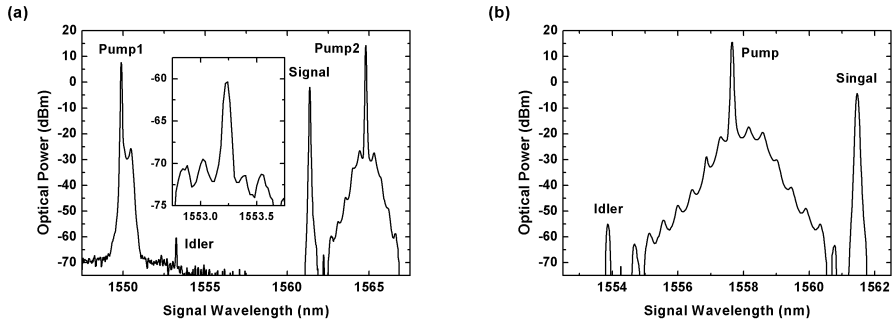

Fig. 2. (a) Optical spectrum of the FWM pumped by two cw pumps at 1549.9 nm and 1564.8 nm. The inset is the enlarged description of the generated idler. (b) Optical spectrum of the FWM pumped by a single cw pump at 1557.7 nm.

By scanning the signal wavelength, the response of conversion efficiency can be obtained from a series of measured FWM spectra, as shown in Fig. 3. It is known that the efficiency is tightly related to the pump powers, i.e., $\eta_{nd} \propto P_{p1}P_{p2}$ and $\eta_d \propto P_p^2$. In the experiments, the gains in the EDFA will be different for the two-pump and single-pump cases. For comparison, unit conversion efficiency is introduced by eliminating the influence of the pump powers (i.e., $\eta_{nd\text{-}unit} = \eta_{nd}/P_{p1}P_{p2}$ and $\eta_{d\text{-}unit} = \eta_d/P_p^2$) [15]. By fitting the measured conversion efficiencies, the experimental bandwidths are calculated from Fig. 3. The bandwidth of the single-pump FWM is 29.8 nm, while it is enhanced to 37.4 nm for the two-pump FWM. The bandwidth is improved by 25% through introducing the two-pump FWM regime.

#137992 - $15.00 USD Received 10 Nov 2010; revised 3 Dec 2010; accepted 6 Dec 2010; published 17 Dec 2010

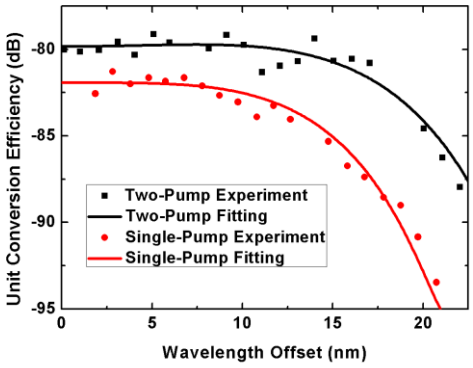

Fig. 3. Measured unit conversion efficiencies and the fitting curves for the two-pump and single-pump wavelength conversions.

3. Simulation verification and discussions

In this section we will verify the experimental results using theoretical simulations. For FWM-based wavelength conversion, the bandwidth is mainly determined by the phase-matching condition. The phase mismatch for the two-pump FWM can be expressed as [17]

$$\kappa = \beta_s + \beta_i - \beta_{p1} - \beta_{p2} + \gamma(P_{p1} + P_{p2}) \tag{1}$$

where $\beta_{p1,p1,s,i}$ are the wave numbers, $P_{p1,p2}$ are the pump powers, and γ is the nonlinear coefficient. In contrast, the single-pump FWM phase mismatch is

$$\kappa = \beta_s + \beta_i - 2\beta_p + 2\gamma P_p \tag{2}$$

where β_p and P_p are the pump wave number and power for the single-pump FWM.

Figure 4(a) shows the calculated dispersion for the silicon waveguide used in the experiment. Using Eqs. (1) and (2), we calculate the phase mismatches for the above experiments in Fig. 4(b) by assuming that the incident pump powers are 11.7 and 18.3 dBm for the two-pump FWM and the pump power is 19.6 dBm for the single-pump FWM according to the measured spectra and the linear and nonlinear losses in the waveguide. Here the wavelength offset represents the deviation of the signal wavelength from the central pump wavelength ($\lambda_{p1}/2 + \lambda_{p2}/2$) in the two-pump FWM or the pump wavelength (λ_p) in the signle-pump FWM. One can see that the phase mismatch is changed by the pump wavelengths in the two-pump FWM because they can be set apart from each other. The minimum phase mismatch is obtained at the wavelength offset of 7.4 nm in the two-pump FWM instead of the zero wavelength offset in the single-pump FWM. The corresponding conversion responses are simulated in Fig. 4(c) by choosing the linear loss coefficient of 0.7 cm^{-1}, the two-photon absorption coefficient of 0.5 cm/GW, and the effective carrier lifetime of 5 ns [19]. It is noticeable that the maximum efficiency emerges corresponding to the minimum phase mismatch, which means a bandwidth enhancement for the two-pump FWM. The bandwidths are calculated to be 36.48 nm and 33.26 nm for the two-pump and single-pump FWMs, respectively. The theoretical simulations agree well with the experimental results. A little deviation may be caused by the difference between the calculated and real dispersions of the waveguide.

#137992 - $15.00 USD Received 10 Nov 2010; revised 3 Dec 2010; accepted 6 Dec 2010; published 17 Dec 2010

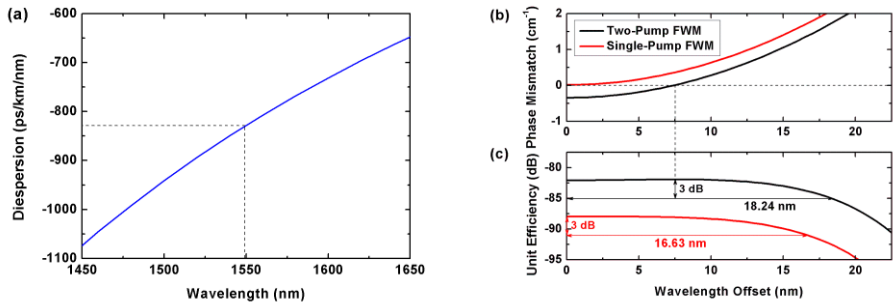

Fig. 4. (a) Dispersion profile of the silicon waveguide used in the experiment and simulation results of (b) the phase mismatch and (c) the corresponding unit conversion efficiency for the two-pump and single-pump FWMs.

Due to the limitations in the tuning range of the filter, the pump spacing cannot be extended in our experiment. However, the bandwidth enhancement can be further improved by increasing the wavelength spacing between the two pumps [17]. In particular, we estimate the bandwidth that can be obtained in the experimental silicon waveguide with the same pump setting as the pump spacing varies, as shown in Fig. 5. The maximum bandwidth is increased to 46.60 nm when the pump spacing is 32.56 nm under the 3-dB nonuniformity. This result provides >40% broader bandwidth than the signal-pump FWM.

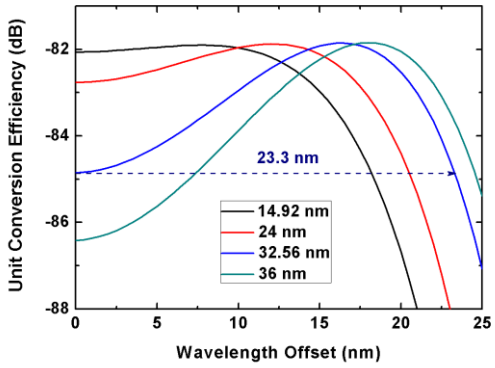

Fig. 5. Unit conversion efficiency versus the wavelength offset for the two-pump FWM in the experimental silicon waveguide with several different pump wavelength spacings.

The measured bandwidth is also limited by the large dispersion value (about –830 ps/km/nm at 1550 nm) of the waveguide we used in the experimental setup. The bandwidth broadens more and the advantage of two-pump regime manifests itself more clearly if a silicon waveguide with low dispersion is used [10]. For instance, for a waveguide width fixed at 650 nm, the dispersion profile will vary as the waveguide height changes. The dispersion values are obtained for waveguide geometries of 300 nm × 650 nm, 285 nm × 650 nm, and 250 nm × 650 nm, respectively, as shown in Fig. 6(a). The zero-dispersion wavelengths for these three waveguide geometries are 1456, 1479, and 1629 nm, and the dispersion values at 1550 nm are 222.5, 148.6, and –70.2 ps/km/nm, respectively. Figure 6(b) shows the enhancement in conversion bandwidth which can be achieved in these three waveguide geometries when the two-pump wavelength conversion is used, where the central pump wavelength is still fixed at 1557.34 nm and the pump wavelength spacing is optimized to achieve the maximum bandwidth under the 3-dB nonuniformity. The free-carrier lifetime is assumed to be 1 ns for these three waveguides. For comparison, the single-pump FWM is also

#137992 - $15.00 USD Received 10 Nov 2010; revised 3 Dec 2010; accepted 6 Dec 2010; published 17 Dec 2010

calculated in these waveguides. The conversion bandwidths are calculated to be 68.5, 83.2, and 114.7 nm for the single-pump FWM in 300 nm × 650 nm, 285 nm × 650 nm, and 250 nm × 650 nm waveguides, which are much broader than what can be obtained in the waveguide we used in our experiment because of their lower dispersion values. Although the bandwidth becomes broader with lower dispersion, the ability of bandwidth enhancement using two-pump FWM is still achievable. In Fig. 6(b), the two-pump bandwidths are 87.9, 106.6, and 165.3 nm, respectively, which show 28.4%, 28.0%, and 44.1% improvement in these waveguides compared to the single-pump FWM. Therefore, the bandwidth enhancement due to two-pump FWM regime as compared to the single-pump FWM is not affected by the dispersion of the silicon waveguide.

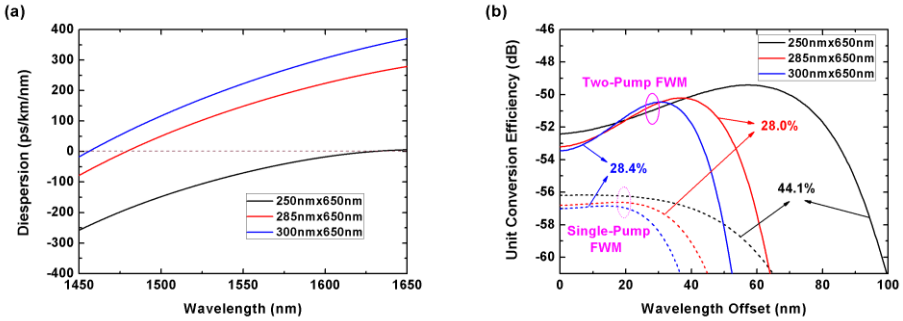

Fig. 6. (a) Dispersion profiles of the silicon waveguide geometries of 300 nm × 650 nm, 285 nm × 650 nm, and 250 nm × 650 nm. (b) Unit conversion efficiency as the wavelength offset varies in the three silicon waveguides, where the solid lines are for the two-pump FWM and the dashed lines are for the single-pump FWM.

4. Conclusion

The wavelength conversion using two-pump FWM has the potential of more controllable and broader conversion bandwidth. We experimentally demonstrate that the enhancement of bandwidth can be as large as 25% in a 17-mm-long silicon waveguide. The experimental results agree well with the theoretical simulations and even >40% improvement can be predicted if the pump spacing is optimized. Although the bandwidth is still limited because the dispersion profile is not optimized for the phase matching of the FWM process, the bandwidth enhancement using two-pump FWM has been verified and the bandwidth enhancement due to two-pump FWM regime as compared to the single-pump FWM is always available in the silicon waveguide with or without dispersion optimization.

Acknowledgements

The authors thank Prof. Ozdal Boyraz (University of California, Irvine) for his valuable discussions. This work was supported by the National Natural Science Foundation of China (Grant Nos. 60708006 and 60978026), the Specialized Research Fund for the Doctoral Program of Higher Education of China (Grant No. 20070335118), and the Zhejiang Provincial Natural Science Foundation of China (Grant No. Y1090379).

#137992 - $15.00 USD Received 10 Nov 2010; revised 3 Dec 2010; accepted 6 Dec 2010; published 17 Dec 2010